

Article

# Multi-Wavelength Polarimetry of Isolated Neutron Stars

Roberto P. Mignani <sup>1,2</sup>

<sup>1</sup> INAF-Istituto di Astrofisica Spaziale e Fisica Cosmica Milano, via E. Bassini 15, 20133 Milano, Italy; mignani@iasf-milano.inaf.it; Tel.: +39-02-23699347

<sup>2</sup> Janusz Gil Institute of Astronomy, University of Zielona Góra, ul. Szafrana 2, 65-516 Zielona Góra, Poland

Received: 29 January 2018; Accepted: 9 March 2018; Published: 13 March 2018

**Abstract:** Isolated neutron stars are known to be endowed with extreme magnetic fields, whose maximum intensity ranges from  $10^{12}$ – $10^{15}$  G, which permeates their magnetospheres. Their surrounding environment is also strongly magnetized, especially in the compact nebulae powered by the relativistic wind from young neutron stars. The radiation from isolated neutron stars and their surrounding nebulae is, thus, supposed to bring a strong polarization signature. Measuring the neutron star polarization brings important information about the properties of their magnetosphere and of their highly magnetized environment. Being the most numerous class of isolated neutron stars, polarization measurements have been traditionally carried out for radio pulsars, hence in the radio band. In this review, I summarize multi-wavelength linear polarization measurements obtained at wavelengths other than radio both for pulsars and other types of isolated neutron stars and outline future perspectives with the upcoming observing facilities.

**Keywords:** neutron star; polarimetry; observations

---

## 1. Introduction

Over 2300 isolated neutron stars (INSs), i.e., not in binary systems, have been identified so far according to the ATNF pulsar catalog [1]. They represent a very important sample where we can study the multi-wavelength emission properties of the neutron star without being affected by the contribution of the companion star, which is dominating at wavelengths such as the optical, infrared or ultraviolet. INSs are known in a variety of flavors, from the classical rotation-powered pulsars (RPPs), either radio-loud or radio-quiet, to the rotating radio transients (RRATs), to the magnetars, the most numerous INS class after the RPPs and powered by the magnetic energy, to the enigmatic central compact objects (CCOs) in supernova remnants (SNRs), to the thermally-emitting INSs (TINSs). The INS fraternity is discussed in the recent review of [2]. Their multi-wavelength phenomenology is very rich and diversified depending on the INS class, going from the RPPs, which can be detected across the entire electromagnetic spectrum, to the CCOs, which are only detected through their thermal emission in the soft X-rays. What makes one INS class different from another is one of the hotly debated issues in compact object astrophysics. Possible explanations point at a difference in the progenitor star, supernova explosion dynamics or early evolution of the new-born neutron star. In some cases, differences in the intrinsic INS properties, such as the magnetic field strength, can help drive the investigations. A clear example is that of the CCOs and the magnetars, both in the same age range (a few kyrs), but with the former being characterized by a magnetic field strength a factor of  $10^4$  lower than the latter.

It is obvious that multi-wavelength observations are key to characterize the INS diversity and determining the cause, possibly placing them in a unique evolutionary path. Polarimetry observations are one of the most important diagnostic tools since they provide, among other things, important

information on the INS magnetosphere properties, allowing one to test different models of NS magnetosphere emission, including the location of the emission regions, and of the INS highly magnetized environment, including their pulsar wind nebulae (PWNe). Since radio pulsars are the most numerous class of INSs, polarization measurements have been traditionally carried out in the radio band, also owing to the difficulties in carrying out polarization measurements at other energies. These arise from the lower photon statistics with respect to the radio band (polarization measurements require high counting rates), from the limited availability of cutting edge detectors and, in the  $\gamma$  and X-rays, from the lack of suitable instruments flying on the majority of space missions. As a matter of fact, apart from the radio band, optical polarimetry observations have been most successful in the study of INSs, exploiting a well-tested technology. In addition, optical observations represent the only way to measure the polarization of INSs that are not detected in the radio band, such as the TINSs, or show, at most, sporadic radio emission, such as the magnetars. It is clear that the information obtained from multi-wavelength polarimetry, from the optical to the  $\gamma$ -rays, complements that obtained from radio polarimetry alone, as it explores incoherent emission processes as opposed to the coherent ones. For this reason, multi-wavelength polarimetry of INSs is crucial for a global understanding and characterization of these objects.

In this review, I will describe the state of the art of multi-wavelength polarimetry observations for different types of INSs carried out outside the radio band, and I will outline future perspectives from the use of new observing facilities that are expected to become operational in the next decade.

## 2. Rotation-Powered Pulsars

As we said above, RPPs represent the most numerous class of INSs, and as such, they offer an ample choice of targets for polarimetry observations. Most importantly, RPPs are the only INS class for which several objects have been observed in different energy bands or even across the entire electromagnetic (non-radio) spectrum, from the infrared (IR), up to the very high-energy  $\gamma$ -rays. For this reason, they are ideal targets for multi-wavelength polarization studies. Indeed, RPPs are the only INS class for which polarization measurements in at least one of these energy bands have been obtained for a few objects and the only INS class for which polarization measurements in multiple energy bands have been obtained for at least one object (a notable case is the Crab pulsar).

### 2.1. RPP Optical Polarimetry

The energy band where most non-radio polarization measurements of RPPs have been obtained so far is the optical band (3000–8000 Å), an important channel to study radio-quiet RPPs. Being the first RPP detected in the optical band [3], as well as due to its brightest ( $V = 16.5$ ), the Crab pulsar (PSR B0531+21) has been the first one for which a measurement of the optical linear polarization<sup>1</sup> has been obtained [4] and the only one for which such measurements, both phase-averaged and phase-resolved, have been obtained through the years with a variety of telescopes/instruments (see [5] and the references therein). Phase-resolved observations (e.g., [6]) have shown that the polarization degree (PD) varies with the phases of the pulsar optical light curve and is maximum in the so-called bridge (BR) region ( $\sim 25\%$ ), the phase interval between the primary and secondary pulse peaks (P1 and P2), and in the off-pulse (OP) region ( $\sim 35\%$ ), the phase interval before the primary peak and after the secondary one, whereas it is minimum in coincidence with the two peaks (a few percent). This suggested the presence of a strong DC component, possibly not associated with the pulsar, but with a second spatially unresolved source. A similar behavior is observed in the near-ultraviolet (UV) thanks to Hubble Space Telescope (HST) phase-resolved polarimetry observations [7], suggesting that the polarization properties in the Crab are not wavelength-dependent, at least in the relatively narrow wavelength range between the optical and near-UV. Why the similarity in the polarization properties

---

<sup>1</sup> In this manuscript, polarization has to be intended as linear polarization unless stated otherwise.

between the optical and the near-UV does not reflect the difference between the optical/near-UV spectrum and light curves [8,9], as one would expect by assuming that the phase-resolved polarization properties depend both on the pulsar spectrum and on the geometry of the emission region, is still to be understood. The optical phase-averaged PD =  $9.8\% \pm 0.1\%$  [6], which becomes  $5.5\% \pm 0.1\%$  after subtracting the DC component. Such a component was suggested [6] to be associated with the compact emission knot seen  $\sim 0.6$  arcsec from the pulsar, resolved by high-spatial resolution imaging with the Hubble Space Telescope (HST), but not in ground-based polarimetry observations. This interpretation has been confirmed by HST polarimetry observations [10,11], which measured a PD of  $59.0\% \pm 1.9\%$  for the knot against a value of  $5.2\% \pm 0.3\%$  measured for the pulsar, perfectly consistent with what was measured from ground-based observations after accounting for the DC component. Quite interestingly, HST observations [11] have shown that the phase-averaged polarization position angle (PA =  $105.1^\circ \pm 1.6^\circ$ ) was approximately aligned with the direction of the pulsar proper motion and with the axis of symmetry of the PWN observed in X-ray by Chandra. A similar alignment was also claimed for the Vela pulsar (PSR B0833–45), based on ground-based observations [12], now confirmed by HST imaging polarimetry measurements [13], and interpreted as evidence of magneto-dynamic interaction between the pulsar and its surrounding environment. The Crab is also the only RPP for which the detection of optical circular polarization has been announced [14], although the actual value has not yet been reported in a publication. As predicted by the recent model of [15], the degree of circular polarization in the optical should be directly dependent on the pulsar magnetic field in the emission region; therefore, measuring circular polarization is a way to constrain the local magnetic field strength.

As of now, there are five RPPs for which a measurement of the optical polarization degree has been obtained, albeit with different levels of significance owing to the different object brightness (see [16], for a recent compilation and reference list). After the Crab, a robust measurement ( $8.1\% \pm 0.7\%$ ) has been obtained for the 11-kyr-old Vela pulsar ( $V = 23.6$ ), with the HST [13]. For the second brightest RPP identified in the optical, the 1.7-kyr-old PSR B0540–69 ( $V = 22.5$ ), the polarization degree has also been obtained with the HST, albeit with discrepant values (5% and 16%), probably owing to a different approach in the subtraction of the PWN contamination and of the foreground polarization along the Large Magellanic Cloud distance (49 kpc). For another young pulsar, PSR B1509–58 (1.7 kyr), only a tentative measurement, 10.4% with no reported error, has been published so far. PSR B0656+14 ( $V = 25$ ) is the only pulsar, apart from the Crab for which both phase-averaged ( $11.9\% \pm 5.5\%$ ) and phase-resolved polarization measurements have been obtained and is also the oldest and faintest one of the sample. From a general point of view, one can see that the optical polarization varies between 5% and 10% and is much lower than measured in the radio bands [17], probably owing to the different emission mechanisms. The observed optical polarization is also a factor of a few lower than expected from predictions based on most pulsar magnetosphere models, although such a discrepancy can be due to over-simplification in the simulation codes or larger than expected depolarization effects in the pulsar magnetosphere (see [12] for a discussion). Bearing its current limitations in mind, the starting sample can be investigated for possible correlations between the polarization degree and the pulsar properties [16]. For instance, a hint of a correlation between PD and the pulsar spin-down age and of anti-correlation with the spin-down energy can be seen, suggesting that the PD is higher for older and less energetic pulsars. At the same time, a possible anti-correlation is seen between PD and the magnetic field at the pulsar light cylinder. Tentative as they might be, these hints can be biased by the fact that PSR B0656+14 is the only pulsar in the sample to occupy certain ranges of the parameter space, e.g., a spin-down age between  $\sim 0.1$  and 1 Myr and a spin-down energy between  $\sim 10^{33}$  and  $10^{35}$  erg  $\text{cm}^{-1} \text{s}^{-1}$ . A more significant measurement of its PD, as well as measuring the PD for other pulsars with similar spin-down parameters (e.g., Geminga), is needed to assess the reality of the observed trends. Apparently, there is no dependence of the PD on the pulsar optical spectral index, suggesting that the way the optical radiation is generated does not obviously affect the level of polarization it can achieve.

Although the current sample is a starting point for future observations, it has to be improved both in quality and quantity, passing through the revision of uncertain cases, such as PSR B1509–58. This is, however, a challenging task owing to the object faintness ( $R \sim 26$ ) and its proximity ( $\sim 0.6$  arcsec) to a four magnitude brighter star, which requires both an 8-m class telescope and a high spatial resolution in the optical. Furthermore, the pulsar is at low latitude with respect to the Galactic plane and at a distance of 4.4 kpc, so that the contribution of the foreground polarization is expected to be dominant. The next best target for phase-averaged optical polarimetry is Geminga ( $V = 25.5$ ), now observed with the VLT (PI : Mignani), especially because of its close distance ( $< 0.3$  kpc), which minimizes the effects of foreground polarization, and it is not surrounded by an optical PWN, which minimizes the polarization background. Furthermore, the spin-down parameters of Geminga are similar to those of PSR B0656+14 [1], which is important to verify the tentative trends observed in [16] between the optical PD and, e.g., the pulsar spin-down age and spin-down energy. Imaging polarimetry of Geminga would also be important to determine whether the alignment between the phase-averaged PD vector and the proper motion direction, seen in the Crab and Vela pulsars [11,13] and, possibly, in PSR B0656+14 [16], is an intrinsic characteristic of RPPs. Being much more informative than phase-average polarization, phase-resolved polarization should be pursued for the brightest targets, i.e., PSR B0540–69 and the Vela pulsar, using recently developed high time polarimetry instruments. Phase-resolved polarimetry would also be crucial to search for possible variations of the pulse PD occurring in coincidence with giant optical pulses, erratic (few percent) variations of the single pulse intensity so far observed in the Crab pulsar only [18,19], and repeating almost exactly in phase with the giant radio pulses, suggesting that the mechanisms that produce giant radio and optical pulses affect both coherent and incoherent radiation emission processes. Both the origin and the connection of giant optical and radio pulses in the Crab are still unclear, but coordinated polarimetry observations in both bands can help to solve the mystery by tracing possible variations in the pulsar magnetosphere properties down to sub-millisecond time scales. Since giant pulses have not yet been detected at X- and  $\gamma$ -ray energies (see, e.g., [20] and the references therein), it is obvious that optical observations are pivotal to this goal. In the future, the detection of giant pulses at X- and  $\gamma$ -ray energies, which might or might not occur in coincidence with giant optical or radio pulses, and the measurement of their polarization would be fundamental to determine whether this phenomenon reflects sudden changes in the entire magnetosphere or only of the regions where emission at a given energy band is produced.

## 2.2. RPP X-Ray Polarimetry

Polarization observations of the Crab Nebula in the X-rays have been carried out since the early 1970s, with the first measurement yielding  $PD = 15.4\% \pm 5.2\%$  in the 5–20-keV energy range [21]. A similar, but more precise value was obtained by [22],  $PD = 15.7\% \pm 1.5\%$ , with the OSO-8 satellite, which was revised to  $19.2\% \pm 1.0\%$  after subtraction of the pulsar contribution [23]. No new measurement had been tried/obtained in the next four decades, mainly owing to the fact that no X-ray polarimeter was flown on the on-orbit or planned X-ray satellites as a result of mission descopeing or cancellation, budget cuts or technical/scientific merit (see Weisskopf on these proceedings for a historical summary). Indeed, with only one object detected, X-ray polarimetry was considered a very risky enterprise, especially in view of the large investment in observing time. Very recently, polarization measurements of the Crab Nebula in the 100–380-keV energy range have been obtained using the Cadmium Zinc Telluride Imager (CZTI) on-board the Indian X-ray satellite ASTROSAT [24]. The phase-averaged PD was found to be  $32.7\% \pm 5.8\%$ , with a PA of  $143.5^\circ \pm 2.8^\circ$ . When phase-resolved, these measurements have shown that the PD is maximum in the OP region (up to  $\sim 80\%$ ) and is still quite high in the BR region ( $\sim 20\%$ ). These results are pretty much in line with what has been already observed in the optical (see, e.g., [6] and the references therein), where the PD is also maximum in the OP and BR regions. In the optical, it has been proposed [6,11] that the high PD measured in the phase interval away from the two peaks is associated with the knot seen close to the pulsar, which is very highly polarized (59%). It is not clear whether the high PD observed in the X-rays in the same

phase intervals is associated with an emission feature in the inner PWN, such as the knot itself, which is unresolved at the Chandra spatial resolution [25], or it is intrinsic to the pulsar. A polarization measurement of the Crab pulsar plus nebula system has been recently obtained with the Pogo+balloon-borne X-ray polarimeter [26] in a close energy range (20–160 keV). Such a measurement could only yield upper limits on the PD of the primary and secondary peaks (73% and 81%, respectively) and of the OP region (37%). The phase-averaged PD, however, was found to be  $20.9\% \pm 5.0\%$ , with a corresponding PA of  $131.3^\circ \pm 6.8^\circ$ , likely dominated by the nebula contribution. For no other RPP has the polarization been measured in the X-rays.

### 2.3. RPP $\gamma$ -Ray Polarimetry

The first polarization measurements of the Crab in the soft  $\gamma$ -ray regime (0.1–1 MeV) were obtained by the Integral satellite. Using the SPI detector, [27] measured a PD of  $46\% \pm 10\%$  in the OP region with a PA =  $123^\circ \pm 11^\circ$ , roughly aligned with the symmetry axis of the PWN. Phase-resolved  $\gamma$ -ray polarization measurements (0.2–0.8 MeV) were also obtained with IBIS, another instrument aboard Integral [28], yielding a PD of  $42_{-16}^{+30}\%$  for the two peaks and of  $>88\%$  for the OP plus BR regions. This showed that, like in the optical [6] and in the X-rays [24], the peaks seem to be much less polarized than the OP plus BR regions. A measurement of the  $\gamma$ -ray polarization in a similar energy range (0.13–0.44 MeV) was also obtained by [29] using Integral/SPI data. Recently, [30] reported on a possible correlated variation of the Crab polarization position angle both in the optical and in the soft  $\gamma$ -rays by comparing multi-epoch measurements obtained with the HST and the Galway Astronomical Stoke Polarimeter (GASP; [31]) at the 5-m Hale Telescope and the Integral/IBIS instrument. More interestingly, these variations seemed to occur in coincidence with high-energy  $\gamma$ -ray flaring events from the Crab Nebula detected by the Fermi satellite. The trend seems to be confirmed by new observations with IBIS and GASP at the 4.2-m William Herschel Telescope [32]. However, GASP observations, let alone the IBIS ones, did not have the angular resolution needed to resolve the pulsar from the nearby knot, so that it was not possible to ascertain which of the two objects, i.e., either the pulsar or the knot, was responsible for the observed polarization PA variability. Quite remarkably, no significant variation of the PD was noticed in parallel to those of the polarization PA [30]. Whether such variations are indeed associated with  $\gamma$ -ray flaring events in the Crab Nebula and whether they are associated either with the pulsar or the knot can be only ascertained by high spatial resolution monitoring polarimetry observations with the HST. Incidentally, reference [30] also reported a measurement of circular polarization ( $-1.2\% \pm 0.4\%$ ) for the pulsar plus knot system. However, also in this case, the GASP angular resolution was not sufficient to spatially resolve the pulsar from the knot and determine their respective contribution to the measured circular polarization. No measurement of linear polarization in the high-energy  $\gamma$ -rays ( $>50$  MeV) has been obtained so far, neither for the Crab, nor for any other RPP. In a recent work, however, reference [33] studied the sensitivity to  $\gamma$ -ray polarization measurements using data from the Fermi Large Area Telescope (LAT) and found that with ten years of data, the LAT could measure a minimum detectable polarization (MDP) of 30–50% at the  $5\sigma$  level for the Crab and Vela pulsar. With Fermi now in its tenth year of operations, and continuing its mission till the end of the decade at least, this is certainly a possibility to be explored in the near future.

### 2.4. Multi-Wavelength Polarimetry

The Crab is the only RPP for which polarization measurements in two, or more, energy bands have been obtained. Some of the most representative values are summarized in Table 1. In most cases, the measurements have been phase-averaged so that it is difficult to separate the contribution of the pulsar from that of the background (the PWN). Only in the optical it has been possible to obtain a neat measurement of the pulsar PD without contamination from nearby sources (i.e., the knot) or the PWN, thanks to the exquisite spatial resolution of the HST. Comparing the PD obtained through different measurements is scientifically interesting, but it is not straightforward owing to possible

observational biases. First of all, owing to the different spatial resolution of the different instruments, such measurements encompass different areas around the pulsar, so that there are different polarization background contributions from the PWN and the SNR. Phase-resolved polarization measurements can provide a direct measurement of the pulsar PD, but they depend on how the BR and OP phase intervals are defined, which might be different from case to case, and rely on the assumption that the pulsar emission is totally pulsed. Finally, being that the Crab PWNe is a highly dynamic environment, the PD might be variable in time, and so its background contribution to the pulsar polarization. Even with these caveats, one might speculate whether the PD is a function of energy. Indeed, looking at the values in Table 1, a hint of a trend for an increase of the PD with energy can be appreciated (see also Figure 4 of [26]), with the ASTROSAT measurement of [24] consistent with such a trend. New measurements, possibly unaffected by observational biases, would be fundamental to confirm such a trend, which, if real, would have important implications on the models of multi-wavelength emission from the pulsar magnetosphere. It is more difficult to recognize a trend in PA, although it seems, on average, larger at higher energies than in the optical. In all cases, however, the PA values are more or less close to the axis of symmetry of the PWN, but not perfectly aligned with each other. Whether the difference in the phase-averaged PAs may reflect a difference in the location of the emission regions and/or in the emission geometry in the NS magnetosphere is unclear.

**Table 1.** Summary of representative multi-wavelength polarization measurements of the Crab pulsar plus nebula, unless otherwise indicated. Columns report the energy range, the phase interval where the polarization has been computed, the polarization degree (PD) and position angle (PA). The last column reports the reference publication. OP, off-pulse; P1, Peak 1; BR, bridge.

Energy range	Phase	PD (%)	PA (°)	Reference
$\gamma$ -ray (0.1–1 MeV)	OP	$46 \pm 10$	$123 \pm 11$	[27]
$\gamma$ -ray (0.2–0.8 MeV)	P1 + P2	$42^{+30}_{-16}$	$70 \pm 20$	[28]
$\gamma$ -ray (0.2–0.8 MeV)	OP	$>72$	$120.6 \pm 8.5$	[28]
$\gamma$ -ray (0.2–0.8 MeV)	OP + BR	$>88$	$122.0 \pm 7.7$	[28]
$\gamma$ -ray (0.2–0.8 MeV)	avg	$47^{+19}_{-13}$	$100 \pm 11$	[28]
$\gamma$ -ray (0.13–0.44 MeV)	avg	$28 \pm 6$	$117 \pm 9$	[29]
X-ray (2.6 keV)	avg	$15.7 \pm 1.5$	$161.1 \pm 2.8$	[22]
X-ray (2.6 keV) <sup>0</sup>	avg	$19.2 \pm 1.0$	$156.4 \pm 1.4$	[23]
X-ray (20–120 keV)	avg	$20.9 \pm 5.0$	$131.3 \pm 6.8$	[26]
X-ray (100–380 keV)	avg	$32.7 \pm 5.8$	$143.5 \pm 2.8$	[24]
Optical <sup>1</sup>	avg	$9.8 \pm 0.1$	$109.5 \pm 0.1$	[6]
Optical <sup>2</sup>	avg	$5.5 \pm 0.1$	$96.4 \pm 0.1$	[10]
Optical <sup>2</sup>	avg	$5.2 \pm 0.3$	$105.1 \pm 1.6$	[11]

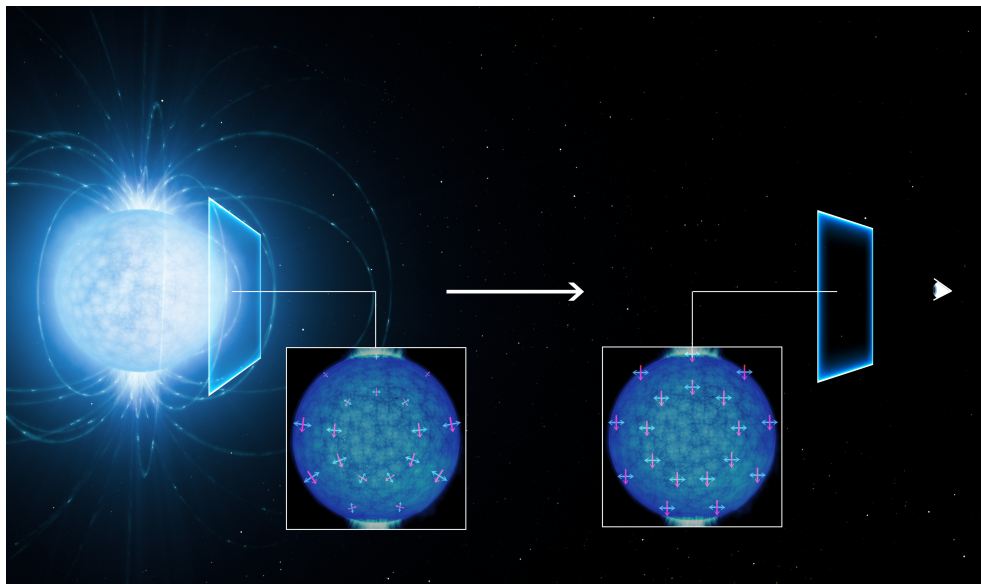
<sup>0</sup> Nebula; <sup>1</sup> pulsar plus knot; <sup>2</sup> pulsar.

### 3. Cooling INSS

While polarization measurements of young RPPs, which are mostly sources of non-thermal radiation, allow one to obtain important information on the neutron star magnetosphere and on the surrounding PWNe, polarization measurements of TINSs allow one to peak directly at, or close to, the NS surface, where their thermal radiation is produced as a result of the star cooling process. In particular, polarization measurements can help addressing several open points on the emission mechanisms of these sources. First of all, it is not clear whether the thermal radiation comes from the bare NS surface or if it is mediated by the presence of an atmosphere. It is also not clear what the composition of such an atmosphere would be and whether and how much it would be magnetized. Furthermore, polarization measurements are also an important tool to test the effects of quantum electrodynamics (QED), which are expected to manifest close to the NS surface, as well as other theories of non-linear electrodynamics (NLED). In particular, vacuum birefringence is expected to increase the level of polarization from the NS surface from a few percent up to 100 percent, depending on the

viewing geometry and the thermal radiation emission mechanism ([34] and the references therein). Thanks to their purely thermal radiation spectrum, TINSs are best suited to test QED effects. Thermal radiation from TINSs is detected in the soft X-rays and in the optical/UV, presumably from regions of different temperatures on the NS surface. However, while their X-ray brightness, as opposed to their optical/UV faintness, would indicate X-ray polarimetry as the most efficient way, no polarimeter working in the soft X-ray range is flying on any of the current X-ray satellites. Therefore, at variance with RPPs, polarimetry measurements of TINSs are only limited to the optical/UV.

Recently, reference [35] observed the TINS RX J1856.5–3754 using an optical imaging polarimeter at the VLT. RX J1856.5–3754 is the brightest (or least faint) INS of this class ( $V = 25.5$ ), and its optical spectral fluxes are best fitted by the Rayleigh–Jeans law, confirming the thermal nature of its radiation. Moreover, it is the closest one, with a parallactic distance of 123 pc only, which minimizes the effect of foreground polarization. The measured optical PD =  $16.43\% \pm 5.26\%$ , which makes RX J1856.5–3754 the faintest INSs for which significant optical polarization has been measured. Unfortunately, the still large statistical errors (much larger than the systematic ones) do not yet allow one to discriminate between different emission models based on the comparison between the predicted and simulated value [35]. Nonetheless, none of the tested thermal emission models (a black body, a magnetized, completely ionized hydrogen atmosphere and a condensed surface) can account for the observed PD unless QED vacuum birefringence effects are included in the simulations, which was assumed by [35] as indirect evidence that vacuum birefringence indeed plays a role in determining the actual value of the PD (Figure 1a,b). Follow-up VLT observations (PI: Mignani) with the same instrument setup have been collected in 2017 for a twice as long integration time, are being analyzed while this manuscript is being written and should provide both a higher significance measurement of the PD and an independent confirmation of the vacuum birefringence effect. RX J1856.5–3754 is, so far, the first and only TINS for which a measurement of the optical polarization has been obtained.



(a)

Figure 1. Cont.

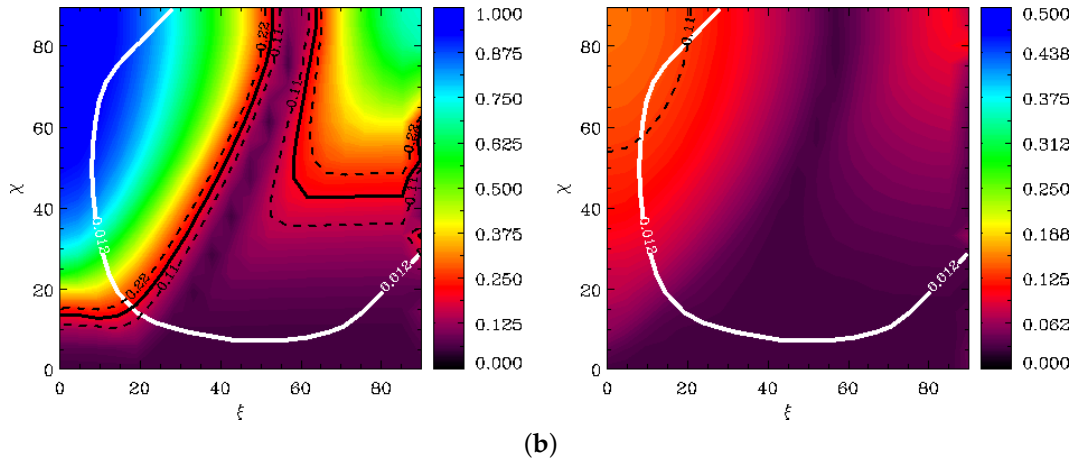


**Figure 1.** (a) Simulation of how the magnetic field affects the light polarization as it propagates away from the neutron star, as predicted by the vacuum birefringence effect. In this case, a distance up to nine neutron star radii has been considered. The blue and red arrows indicate the electric and magnetic field vectors, respectively (image credit ESO). As can be seen, the vector orientation changes with the distance from the neutron star surface, and so does the light polarization. (b) Simulated PD of RX J1856.5–3754 (in color scale) as a function of the angles  $\chi$  and  $\zeta$ , i.e., between the line of sight and the isolated neutron star (INS) spin axis and between the INS magnetic and spin axis, respectively. A black body emission model is assumed in the case shown here. The white solid line represents the constraints on  $\chi$  and  $\zeta$  inferred from the pulsed X-ray light curve (see [35] for details), whereas the black solid line corresponds to the VLT optical polarization measurement [35], including  $1\sigma$  errors (black dashed line). The plots on the left and on the right represent the cases when QED effects are and are not accounted for, respectively (adapted from [35]).

#### 4. Magnetars

Magnetars are the only remaining class of INSs for which polarization measurements outside the radio bands have been obtained in at least one case. Being extremely magnetized objects, with magnetic fields up to three orders of magnitude above that of the Crab pulsar, the radiation from the magnetar magnetosphere is expected to be highly polarized. Furthermore, magnetars are the most variable class of INSs, featuring bursts, outbursts and giant flares, where the flux can vary up to several orders of magnitude (see [36], for a review). Therefore, they are spectacular laboratories for testing the magnetic field evolution after or during one of such events, and polarimetry represents one of the most useful diagnostic tools. Having a thermal X-ray spectrum harder than the TINSs, with the addition of non-thermal X-ray components detected up to  $\sim 100$  keV, magnetars can be targets of X-ray polarimetry observations. However, no measurement has been obtained with any of the current hard X-ray observing facilities, such as Integral. Magnetars, however, have also been detected in the optical/IR, where the emission is non-thermal and, possibly, powered by the magnetic field, as suggested by the higher fraction of their spin-down power converted into optical/IR luminosity with respect to RPPs [37]. While they are usually intrinsically very faint in quiescence and affected by a large interstellar extinction owing to their location on the Galactic plane and distances of a few kpc, magnetars can become relatively bright when they are in outburst.

Phase-averaged imaging polarimetry observations in the IR have been carried out for some magnetars using the VLT (Israel et al., in preparation). For both 1E 1048–5937 and XTE J1810–197, only an upper limit of 25% on the PD has been obtained. For a third magnetar, 1E 1547.0–5408, follow-up observations of its IR counterpart, identified after an outburst onset [38], yielded a PD value of  $4.2\% \pm 0.9\%$ . This is the first measurement of a magnetar PD outside the radio band. However, the contribution of the foreground polarization at the magnetar  $\sim 5$  kpc distance ( $A_K \sim 1.9$ ) is the largest source of uncertainty, which makes this value still preliminary. If correct, the measured PD might

sound somehow lower than one would expect for an highly-magnetized object, like 1E 1547.0–5408 ( $B = 2.2 \times 10^{14}$  G). However, at least in the case of RPPs, no dependence has been found between the PD and the NS surface magnetic field [16], although the explored magnetic field range is relatively narrow ( $B = 3.4 \times 10^{12} - 1.54 \times 10^{13}$  G). The PD measured for 1E 1547.0–5408 is somewhat lower than the average for RPPs, which has been obtained in the optical (V band). No polarization measurement in the IR has been obtained yet for any RPP that can be taken for comparison, however, so that we cannot rule out that the PD is wavelength dependent and lower in the IR than in the optical. An upper limit on the circular polarization of 4.3% has been obtained in the optical for the magnetar 4U 0142–61 with the Subaru telescope [39] and is the only one reported so far for an INS of this type. The measurement of circular polarization in magnetars can, in principle, help to discriminate between different emission models of magnetars' optical emission, e.g., synchrotron/curvature radiation from electron/positron pairs or ion cyclotron radiation (see the discussion in [39] and the references therein). An upper limit of 4.3% on the circular polarization might rule out synchrotron/curvature radiation, but might still be compatible with ion cyclotron radiation, although [39] note that their measurement is still too uncertain and model predictions still too vague to make any strong claim.

## 5. Future Perspectives

In total, there are seven INSs (five RPPs, one TINS, one magnetar) for which a polarization measurement has been obtained outside the radio band, i.e., in the optical/UV/IR, and one (the Crab pulsar) with a polarization measurement also in the X-rays/soft  $\gamma$ -rays. In this section, I describe the future perspectives for observations of these INS classes at optical, X- and  $\gamma$ -ray wavelengths with the upcoming facilities.

### 5.1. Optical

Being the INS class with more identifications in the optical domain (about a dozen plus three candidates [40]), polarization measurements of RPPs comprise one of the goals to be pursued with the current facilities. ESO observing programs to obtain phase-resolved polarization measurements of PSR B0540–69 and the Vela pulsar at the 3.6-m telescope with the GASP instrument (PI: Shearer) and phase-averaged measurements of Geminga at the VLT (PI: Mignani) have been approved, and the observations are now being carried out or completed. Follow-up phase-resolved observations for PSR B0656+14 and, possibly, Geminga should also be pursued depending on the possibility of hosting guest instruments, such as GASP, at 8-m class telescopes, either at Northern or Southern Hemisphere telescopes. For some of the remaining targets, polarimetry observations are complicated by the proximity to nearby stars (e.g., PSR B1509–58, PSR B1055–52 and PSR J1751–2054), whereas for the faintest ones, with fluxes fainter than magnitude 26, we would require very large integrations (a few tens of hours) with 8-m class telescopes and very good and stable seeing conditions in dark time to maximize the signal-to-noise, which are difficult to match in ground-based observatories. The same is true for the TINSs, which are all fainter than RX J1856.4–3754 in the optical. The perspective is a bit more promising for magnetars, which can be relatively bright in outburst, but polarimetry observations must be realized with a quick response time to observe the source at the brightness peak and still have to cope with the problem of foreground polarization. In the forthcoming future, observations with the 30–40-m class telescopes, such as the ESO ELT, might provide the required collecting power and spatial resolution. However, at least according to current plans, no polarimeter should be among the first generation instruments. Moreover, in the case of the ELT, multiple reflections in the mirror system would increase the instrument polarization, making it difficult to calibrate it out. The plans for the VLT after 2025, however, are still unclear, but it is desirable that the advent of the ELT will trigger a rethinking of the scientific priorities of the Paranal Observatory, offering the opportunity to mount (semi-)permanent optical polarization instruments. The HST is an ideal telescope for high-spatial resolution imaging observations, and it would play a crucial role in searching for changes of polarization of the Crab pulsar plus knot system in coincidence with  $\gamma$ -ray flares [30,32],

disentangling the contribution of the two components and helping to solve the long-standing mystery on the origin of such events.

### 5.2. X-Rays

With the Crab pulsar being the only INSs for which X-ray polarization measurements have been obtained, it is obvious that X-ray polarimetry is a resource largely unexplored. Perspectives will change in the coming decade with the deployment of new observing facilities dedicated to X-ray polarimetry observations, such as NASA's Imaging X-ray Polarimeter Explorer (IXPE; [41]) a SMEX-class mission due to fly in the early 2020s, ESA's X-ray Imaging Polarimeter Explorer (XIPE; [42]), a candidate medium-class mission with a launch window in the mid-2020s<sup>2</sup>, and the enhanced X-ray Timing Polarimetry mission (eXTP; [43]), a Chinese project with European partner institutions already approved by the Chinese Academy of Science and due to fly around 2025. These three missions are based on the gas pixel detector (GPD) technology and have been designed to work in roughly the same energy range (2–8 keV or 2–10 keV), with a similar field of view ( $\sim 12 \times 12$  arcmin), with a time resolution better than 100  $\mu$ s (XIPE's would be better than 8  $\mu$ s), although with different effective areas, with that of both XIPE and eXTP being about twice as high that of IXPE. This translates to a minimum detectable polarization (MDP) between  $\sim 1\%$  and  $\sim 2\%$  for the same flux limit ( $2 \times 10^{-10}$  erg cm<sup>-2</sup> s<sup>-1</sup> = 10 mCrab) and integration time (300 ks).

Owing to the energy range, only RPPs and magnetars will be suitable targets for these missions (see Taverna and Turolla, these proceedings, for a discussion of the magnetar case). The brightest target RPPs are also embedded in bright X-ray PWNe, which represent a major source of background polarization that cannot be easily subtracted owing to the coarse angular resolution of the GPD detectors (<30 arcsec), which, in most cases, is larger than the angular dimension of the PWN. Moreover, X-ray PWNe are also known to vary in flux (e.g., the Crab and Vela PWNe), and so might be the polarization background, although flux changes do not necessarily come together with changes in the polarization level, at least this is the case in the optical [11]. While for compact pulsar/PWNe systems, targets can be selected by requiring that the PWN X-ray flux does not exceed a certain fraction of the pulsar flux, it has to be noted that a low X-ray flux does not necessarily imply a low polarization level. Therefore, since most of the best-suited target RPPs, selected on the basis of their 2–10-keV flux and corresponding MDP, are also X-ray pulsars in this energy band, the best approach would be to exploit the GPD time resolution to isolate the pulsar contribution (pulsed) from that of the PWN (unpulsed) through phase-resolved polarimetry. While no dedicated mission has been approved yet, concept studies for X-ray polarimeters working in the soft X-ray band (0.1–2 keV) are being carried out, with prototypes to be tested on suborbital flights (see Marshall et al., these proceedings). Extending the sensitivity range of X-ray polarimetry would be fundamental to study TINSs, for which polarization measurements in the optical domain are challenging owing to the target faintness. Measurements of the X-ray PD would be crucial to complement, and test on a larger sample, the results on vacuum birefringence already obtained in the optical [35] and verify the predicted dependence of this effect on the photon energy.

### 5.3. $\gamma$ -Rays

While Integral will still be operational for the next few years and will likely be used to continue its monitoring of the Crab pulsar in the soft  $\gamma$ -rays and Fermi might allow measuring polarization in the high-energy  $\gamma$ -rays at least for the Crab and Vela pulsar [33], it is clear that a major step forward in INS studies must rely on a new observing facility with breakthrough capabilities for  $\gamma$ -ray polarimetry. The e-ASTROGAM satellite [44], a candidate mission for  $\gamma$ -ray astrophysics in the 0.15 MeV–3-GeV energy range, now being evaluated for the ESA M5 selection, satisfies these

<sup>2</sup> At the time of writing, the official selection of the ESA medium-class mission for Cycle 4 (M4) has not been announced yet.

requirements. e-ASTROGAM would be able to carry out polarization measurements through the pair creation and Compton scattering techniques, allowing one to achieve an MDP as low as 1% in the low-energy range (0.2–2 MeV) for a Crab-like source with a 1-Ms integration [45]. Other RPPs detected at low-energy  $\gamma$ -rays by the COMPTEL instrument aboard the Compton Gamma-ray Observatory would also be prime targets for polarimetry observations with e-ASTROGAM [46]. The PWN polarization contamination problem would likely be more severe than in the X-rays and cannot be directly subtracted through background sampling owing to the coarser spatial resolution in the  $\gamma$ -rays. Therefore, target selection criteria might be different and, presumably, mostly based on photon selection from the  $\gamma$ -ray light curve analysis. Like in the X-rays, the advent of this mission would open the so far barely explored field of INS  $\gamma$ -ray polarimetry.

## 6. Conclusions

Polarization studies of INSs are still in their infancy, with very few objects (mostly RPPs) with a polarization measurement outside the radio band, typically in the optical. This is especially true at high energies where only for the Crab pulsar it has been possible to measure polarization both in the hard X-rays and in the soft  $\gamma$ -rays. Even these very few detections, however, have shown the potentials of the diagnostic power of polarimetry in the field of pulsar electrodynamics, e.g., by testing INS magnetosphere and emission models, and in quantum physics, e.g., by verifying QED predictions, such as vacuum birefringence, which built a new bridge between the astrophysics and fundamental physics communities. Times are, thus, mature to carry out polarization studies of INSs on a larger scale, capitalizing on the momentum built in the astronomical community. The blossoming of proposed/planned observing facilities dedicated to, or capable of, polarimetry observations at high energies witnesses this change. These new facilities will expand by a factor of ten to twenty the number of INSs with detected polarized high-energy emission, opening scientific horizons unforeseen till now. From a general stand point, multi-wavelength polarization measurements will allow one to study the properties of INS magnetic fields and magnetospheres in different energy regimes, verify the dependence of the polarization level on the photon energy and the INS spectrum for the first time and disentangle different emission mechanisms, for which different polarization signatures are expected. Together with the information from multi-wavelength timing and spectroscopy, this will make it possible to attack in a systematic way the physics of radiation emission from the neutron star magnetosphere and surface. In particular, as shown by [34,47], the measurement of the degree of polarization from the thermal radiation from a neutron star magnetized hydrogen atmosphere encodes information on the neutron star mass-to-radius ratio, which is a crucial ingredient to test different models of the NS equation of state. With IXPE, eXTP and XIPE, in the X-rays, eASTROGAM in the  $\gamma$ -rays, if approved, and hopefully dedicated instruments at future optical facilities (ELTs), in the mid-2020s, we will enter a new era of multi-wavelength polarimetry, adding a fourth technique, after imaging, timing and spectroscopy, for the multi-wavelength study of INSs.

**Acknowledgments:** The author acknowledges financial support from an INAF Occhialini Fellowship and thanks the two anonymous referees for their constructive comments to the manuscript.

**Conflicts of Interest:** The author declares no conflict of interest. The founding sponsors had no role in the design of the study; in the collection, analyses or interpretation of data; in the writing of the manuscript; nor in the decision to publish the results.

## References

1. Manchester, R.N.; Hobbs, G.B.; Teoh, A.; Hobbs, M. The Australia Telescope National Facility Pulsar Catalogue. *Astron. J.* **2005**, *129*, 1993–2006.
2. Harding, A.K. The neutron star zoo. *Front. Phys.* **2013**, *8*, 679–692.
3. Cocke, W.J.; Disney, M.J.; Taylor, D.J. Discovery of Optical Signals from Pulsar NP 0532. *Nature* **1969**, *221*, 525–527.

4. Wampler, E.J.; Scargle, J.D.; Miller, J.S. Optical Observations of the Crab Nebula Pulsar. *Astrophys. J.* **1969**, *157*, L1.
5. Mignani, R. The Crab Optical and UV Polarimetry. In Proceedings of the Polarimetry days in Rome: Crab Status, Theory and Prospects, Rome, Italy, 16–17 October 2008; p. 9.
6. Słowikowska, A.; Kanbach, G.; Kramer, M.; Stefanescu, A. Optical polarization of the Crab pulsar: Precision measurements and comparison to the radio emission. *Mon. Not. R. Astron. Soc.* **2009**, *397*, 103–123.
7. Graham-Smith, F.; Dolan, J.F.; Boyd, P.T.; Biggs, J.D.; Lyne, A.G.; Percival, J.W. The ultraviolet polarization of the Crab pulsar. *Mon. Not. R. Astron. Soc.* **1996**, *282*, 1354–1358.
8. Sollerman, J.; Lundqvist, P.; Lindler, D.; Chevalier, R.A.; Fransson, C.; Gull, T.R.; Pun, C.S.J.; Sonneborn, G. Observations of the Crab Nebula and Its Pulsar in the Far-Ultraviolet and in the Optical. *Astrophys. J.* **2000**, *537*, 861–874.
9. Percival, J.W.; Biggs, J.D.; Dolan, J.F.; Robinson, E.L.; Taylor, M.J.; Bless, R.C.; Elliot, J.L.; Nelson, M.J.; Ramseyer, T.F.; van Citters, G.W.; Zhang, E. The Crab pulsar in the visible and ultraviolet with 20 microsecond effective time resolution. *Astrophys. J.* **1993**, *407*, 276–283.
10. Słowikowska, A.; Mignani, R.; Kanbach, G.; Krzeszowski, K. Decomposition of the Optical Polarisation Components of the Crab Pulsar and its Nebula. In *Electromagnetic Radiation from Pulsars and Magnetars, Proceedings of a Conference held at University of Zielona Góra, Zielona Góra, Poland, 24–27 April 2012*; Lewandowski, W., Maron, O., Kijak, J., Eds.; Astronomical Society of the Pacific: San Francisco, CA, USA, 2012; Volume 466, p. 37.
11. Moran, P.; Shearer, A.; Mignani, R.P.; Słowikowska, A.; De Luca, A.; Gouiffès, C.; Laurent, P. Optical polarimetry of the inner Crab nebula and pulsar. *Mon. Not. R. Astron. Soc.* **2013**, *433*, 2564–2575.
12. Mignani, R.P.; Bagnulo, S.; Dyks, J.; Lo Curto, G.; Słowikowska, A. The optical polarisation of the Vela pulsar revisited. *Astron. Astrophys.* **2007**, *467*, 1157–1162.
13. Moran, P.; Mignani, R.P.; Shearer, A. HST optical polarimetry of the Vela pulsar and nebula. *Mon. Not. R. Astron. Soc.* **2014**, *445*, 835–844.
14. Wiktorowicz, S.; Ramirez-Ruiz, E.; Illing, R.M.E.; Nofi, L. Discovery of Optical Circular Polarization of the Crab Pulsar. In *American Astronomical Society Meeting Abstracts*; American Astronomical Society: Washington, DC, USA, 2015; Volume 225.
15. De Búrca, D.; Shearer, A. Circular polarization of synchrotron radiation in high magnetic fields. *Mon. Not. R. Astron. Soc.* **2015**, *450*, 533–540.
16. Mignani, R.P.; Moran, P.; Shearer, A.; Testa, V.; Słowikowska, A.; Rudak, B.; Krzeszowski, K.; Kanbach, G. VLT polarimetry observations of the middle-aged pulsar PSR B0656+14. *Astron. Astrophys.* **2015**, *583*, A105.
17. Weltevrede, P.; Johnston, S. Profile and polarization characteristics of energetic pulsars. *Mon. Not. R. Astron. Soc.* **2008**, *391*, 1210–1226.
18. Shearer, A.; Stappers, B.; O’Connor, P.; Golden, A.; Strom, R.; Redfern, M.; Ryan, O. Enhanced Optical Emission During Crab Giant Radio Pulses. *Science* **2003**, *301*, 493–495.
19. Strader, M.J.; Johnson, M.D.; Mazin, B.A.; Spiro Jaeger, G.V.; Gwinn, C.R.; Meeker, S.R.; Szypryt, P.; van Eyken, J.C.; Marsden, D.; O’Brien, K.; et al. Excess Optical Enhancement Observed with ARCONS for Early Crab Giant Pulses. *Astrophys. J.* **2013**, *779*, L12.
20. Hitomi Collaboration; Aharonian, F.; Akamatsu, H.; Akimoto, F.; Allen, S.W.; Angelini, L.; Audard, M.; Awaki, H.; Axelsson, M.; Bamba, A.; et al. Hitomi X-ray studies of Giant Radio Pulses from the Crab pulsar. *arXiv* **2017**, arXiv:1707.08801.
21. Novick, R.; Weisskopf, M.C.; Berthelsdorf, R.; Linke, R.; Wolff, R.S. Detection of X-Ray Polarization of the Crab Nebula. *Astrophys. J.* **1972**, *174*, L1.
22. Weisskopf, M.C.; Cohen, G.G.; Kestenbaum, H.L.; Long, K.S.; Novick, R.; Wolff, R.S. Measurement of the X-ray polarization of the Crab Nebula. *Astrophys. J.* **1976**, *208*, L125–L128.
23. Weisskopf, M.C.; Silver, E.H.; Kestenbaum, H.L.; Long, K.S.; Novick, R. A precision measurement of the X-ray polarization of the Crab Nebula without pulsar contamination. *Astrophys. J.* **1978**, *220*, L117–L121.
24. Vadawale, S.V.; Chattopadhyay, T.; Mithun, N.P.S.; Rao, A.R.; Bhattacharya, D.; Vibhute, A.; Bhalerao, V.B.; Dewangan, G.C.; Misra, R.; Paul, B.; et al. Phase-resolved X-ray polarimetry of the Crab pulsar with the AstroSat CZT Imager. *Nat. Astron.* **2018**, *2*, 50–55.

25. Rudy, A.; Horns, D.; DeLuca, A.; Kolodziejczak, J.; Tennant, A.; Yuan, Y.; Buehler, R.; Arons, J.; Blandford, R.; Caraveo, P.; et al. Characterization of the Inner Knot of the Crab: The Site of the Gamma-Ray Flares? In *American Astronomical Society Meeting Abstracts*; The American Astronomical Society: Washington, DC, USA, 2015; Volume 811, p. 24.
26. Chauvin, M.; Florén, H.G.; Friis, M.; Jackson, M.; Kamae, T.; Kataoka, J.; Kawano, T.; Kiss, M.; Mikhalev, V.; Mizuno, T.; et al. Shedding new light on the Crab with polarized X-rays. *Sci. Rep.* **2017**, *7*, 7816.
27. Dean, A.J.; Clark, D.J.; Stephen, J.B.; McBride, V.A.; Bassani, L.; Bazzano, A.; Bird, A.J.; Hill, A.B.; Shaw, S.E.; Ubertini, P. Polarized Gamma-Ray Emission from the Crab. *Science* **2008**, *321*, 1183.
28. Forot, M.; Laurent, P.; Grenier, I.A.; Gouiffès, C.; Lebrun, F. Polarization of the Crab Pulsar and Nebula as Observed by the INTEGRAL/IBIS Telescope. *Astrophys. J.* **2008**, *688*, L29.
29. Chauvin, M.; Roques, J.P.; Clark, D.J.; Jourdain, E. Polarimetry in the Hard X-Ray Domain with INTEGRAL SPI. *Astrophys. J.* **2013**, *769*, 137.
30. Moran, P.; Kyne, G.; Gouiffès, C.; Laurent, P.; Hallinan, G.; Redfern, R.M.; Shearer, A. A recent change in the optical and  $\gamma$ -ray polarization of the Crab nebula and pulsar. *Mon. Not. R. Astron. Soc.* **2016**, *456*, 2974–2981.
31. Collins, P.; Kyne, G.; Lara, D.; Redfern, M.; Shearer, A.; Sheehan, B. The Galway astronomical Stokes polarimeter: An all-Stokes optical polarimeter with ultra-high time resolution. *Exp. Astron.* **2013**, *36*, 479–503.
32. Gouiffès, C.; Laurent, P.; Shearer, A.; O'Connor, E.; Moran, P. New hard X-rays and optical polarimetric observations of the Crab nebula and pulsar. In *Proceedings of the 11th INTEGRAL Conference Gamma-Ray Astrophysics in Multi-Wavelength Perspective*, Amsterdam, The Netherlands, 10–14 October 2016; p. 38. Available online: <https://pos.sissa.it/285/> (accessed on 8 March 2018).
33. Giomi, M.; Bühler, R.; Sgrò, C.; Longo, F.; Atwood, W.B. Estimate of the Fermi large area telescope sensitivity to gamma-ray polarization. In *Proceedings of the 6th International Symposium on High Energy Gamma-Ray Astronomy*, Heidelberg, Germany, 11–15 July 2016; American Institute of Physics Conference Series; AIP Publishing: College Park, MD, USA, 2017; Volume 1792.
34. Heyl, J.S.; Shaviv, N.J.; Lloyd, D. The high-energy polarization-limiting radius of neutron star magnetospheres—I. Slowly rotating neutron stars. *Mon. Not. R. Astron. Soc.* **2003**, *342*, 134–144.
35. Mignani, R.P.; Testa, V.; González Caniulef, D.; Taverna, R.; Turolla, R.; Zane, S.; Wu, K. Evidence for vacuum birefringence from the first optical-polarimetry measurement of the isolated neutron star RX J1856.5-3754. *Mon. Not. R. Astron. Soc.* **2017**, *465*, 492–500.
36. Turolla, R.; Zane, S.; Watts, A.L. Magnetars: The physics behind observations. A review. *Rep. Prog. Phys.* **2015**, *78*, 116901.
37. Mignani, R.P.; Perna, R.; Rea, N.; Israel, G.L.; Mereghetti, S.; Lo Curto, G. VLT/NACO observations of the high-magnetic field radio pulsar PSR J1119-6127. *Astron. Astrophys.* **2007**, *471*, 265–270.
38. Israel, G.L.; Rea, N.; Rol, E.; Mignani, R.; Testa, V.; Stella, L.; Esposito, P.; Mereghetti, S.; Tiengo, A.; Marconi, G.; et al. ESO-VLT discovery of the variable nIR counterpart to the AXP 1E1547.0-5408. *The Astronomer's Telegram*, January 2009.
39. Wang, Z.; Tanaka, Y.T.; Zhong, J. Subaru Constraint on Circular Polarization in I-Band Emission from the Magnetar 4U 0142+61. *Publ. Astron. Soc. Jpn.* **2012**, *64*, L1.
40. Mignani, R.P. Optical, ultraviolet, and infrared observations of isolated neutron stars. *Adv. Space Res.* **2011**, *47*, 1281.
41. Weisskopf, M.C.; Ramsey, B.; O'Dell, S.; Tennant, A.; Elsner, R.; Soffitta, P.; Bellazzini, R.; Costa, E.; Kolodziejczak, J.; Kaspi, V.; et al. The Imaging X-ray Polarimetry Explorer (IXPE). In *Space Telescopes and Instrumentation 2016: Ultraviolet to Gamma Ray*; SPIE: Bellingham, WA, USA, 2016; Volume 9905.
42. Soffitta, P.; Bellazzini, R.; Bozzo, E.; Burwitz, V.; Castro-Tirado, A.; Costa, E.; Courvoisier, T.; Feng, H.; Gburek, S.; Goosmann, R.; et al. XIPE: The x-ray imaging polarimetry explorer. In *Space Telescopes and Instrumentation 2016: Ultraviolet to Gamma Ray*; SPIE: Bellingham, WA, USA, 2016; Volume 9905.
43. Zhang, S.N.; Feroci, M.; Santangelo, A.; Dong, Y.W.; Feng, H.; Lu, F.J.; Nandra, K.; Wang, Z.S.; Zhang, S.; Bozzo, E.; et al. eXTP: Enhanced X-ray Timing and Polarization mission. In *Space Telescopes and Instrumentation 2016: Ultraviolet to Gamma Ray*; SPIE: Bellingham, WA, USA, 2016; Volume 9905.
44. De Angelis, A.; Tatischeff, V.; Tavani, M.; Oberlack, U.; Grenier, I.; Hanlon, L.; Walter, R.; Argan, A.; von Ballmoos, P.; Bulgarelli, A.; et al. The e-ASTROGAM mission. Exploring the extreme Universe with gamma rays in the MeV–GeV range. *Exp. Astron.* **2017**, *44*, 25–82.

45. Tatischeff, V.; De Angelis, A.; Gouiffès, C.; Hanlon, L.; Laurent, P.; Madejski, G.; Tavani, M.; Ulyanov, A. e-ASTROGAM mission: A major step forward for gamma-ray polarimetry. *arXiv* **2017**, arXiv:1706.07031.
46. De Angelis, A.; Tatischeff, V.; Grenier, I.A.; McEnery, J.; Mallamaci, M.; Tavani, M.; Oberlack, U.; Hanlon, L.; Walter, R.; Argan, A.; et al. Science with e-ASTROGAM (A space mission for MeV-GeV gamma-ray astrophysics). *arXiv* **2017**, arXiv:1711.01265.
47. Heyl, J.S.; Lloyd, D.; Shaviv, N.J. The High-Energy Polarization-Limiting Radius of Neutron Star Magnetospheres II—Magnetized Hydrogen Atmospheres. *arXiv* **2005**, arXiv:0502351.



© 2018 by the author. Licensee MDPI, Basel, Switzerland. This article is an open access article distributed under the terms and conditions of the Creative Commons Attribution (CC BY) license (<http://creativecommons.org/licenses/by/4.0/>).